Effect of temperature and strain on the formation of elongated fine grained structure in middle carbon steel during large plastic deformation

2014 IOP Conf. Ser.: Mater. Sci. Eng. 63 012054

(http://iopscience.iop.org/1757-899X/63/1/012054)

IOP Conf. Series: Materials Science and Engineering **63** (2014) 012054 doi:10.1088/1757-899X/63/1/012054

Effect of temperature and strain on the formation of elongated fine grained structure in middle carbon steel during large plastic deformation

O K Dedyulina, N D Stepanov, G A Salishchev

Laboratory of Bulk Nanostructured Materials, Belgorod State University, 85 Pobeda Str., Belgorod, 803015, Russia
E-mail: dedyulina@bsu.edu.ru

The influence of deformation temperature and strain rate on the mechanisms of elongated fine grain (EFG) formation in the medium-carbon steel was studied. Compression tests were carried out at the temperatures in range of 673-973K at three different strain rates: 10^{-2}, $1.3*10^{-3}$ and 10^{-4} s^{-1}. Presence of two temperature intervals with different dominant mechanisms of deformation was identified: low temperature (673-823K) interval and high temperature (873-973K) interval. Microstructure evolution during deformation at strain rate of $1.3*10^{-3}$ s^{-1} and different temperatures was studied. Also was investigated the microstructure and mechanical properties of steel after warm plastic deformation. EFG structure formation in steel by caliber rolling at temperatures 673 and 773K on strain $\varepsilon \sim 1.1$ results in a significant increase of toughness, including at low temperatures, while improving strength.

1. Introduction

Formation of elongated fine grained (EFG) structure is one of a promising way to reach simultaneous increase in strength and toughness of materials [1, 2]. In particular, in carbon steels, which are widely used in industry due to their low cost and high performance, EFG structure considerably enhances toughness even in the temperature interval of ductile-brittle transition [3-5]. Different large plastic deformation methods can be used to obtain EFG structure in carbon steels [2]. Deformation should be carried out at temperatures of ferrite-cementite field since fine carbide particles are helpful for suppressing grain coarsening during deformation at elevated temperatures, where hard and brittle martensite transforms into ductile ferrite. Combination of fine soft ferritic grains and hard cementite particles promotes good balance of strength and toughness. By varying processing conditions such as temperature and strain structures with different thickness of elongated grains and fraction of high angle boundaries can be obtained. It opens the way to control the mechanical properties.

Recrystallization kinetic and structure formation during hot deformation of medium-carbon steels in the austenitic region were examined by many researchers [6-8]. Upon deformation at low temperatures the development of structure is believed to be controlled by two processes: geometrical effect of strain and dynamic recrystallization. However, this issue has not been studied up to the end relative to medium-carbon steel. Therefore the aim of this paper is to study the mechanisms of EFG structure formation in temperature range 673-973K in the medium-carbon steel and then to explore its mechanical properties.

2. Experimental Procedure

The material used in this study was medium-carbon steel, which chemical composition listed in Table 1. Compression test specimens of 10 x 10 x 12 and 8 x 8 x 10 mm size were cut from the as-received hot rolled bar by electric-discharge machine. All these specimens were heated to 1133K and quenched to produce martensitic structure. The compression tests were conducted using a testing machine Instron 300XL equipped with radial heating furnace. The specimens were first heated up to the deformation temperature and held for 10 min prior to straining. Compression tests were carried out at temperatures in range of 673-973K in 50K steps (seven different temperatures) and at three different strain rates (10^{-2}, $1.3*10^{-3}$ and 10^{-4} s^{-1}). Microstructure evolution was investigated after compression tests at temperatures in range of 673-973K in 100K steps (four different temperatures) and $1.3*10^{-3}$ s^{-1} strain rate continued to true strain $\varepsilon \sim 0.3$, 0.77 and 1.15. For mechanical properties study quenched rod with of Ø20x200 mm size was subjected to caliber rolling at temperatures 773 and 873K and strain $\varepsilon \sim 1.1$.

Microstructure was characterized by electron back scattering diffraction (EBSD) maps on the microscope Nova Nanosem 450 equipped with an orientation imaging microscopy (OIM) system. The EBSD maps size was 20 x 20 μm and 45 x 45 μm and for specimens after caliber rolling – 25 x 25 μm. The step size was 50 nm. In the EBSD maps high angle boundaries (HAB) are shown by black lines and have misorientations $\geq 15^{o}$, while low angle boundaries are depicted by white lines and have misorientations $< 15^{o}$.

The tensile tests were conducted using the Instron 5882 mechanical testing machine at room temperature. Cylindrical specimens with a gauge length of 25 mm and a diameter of 5 mm were used. Impact tests were carried out at temperatures from 77 to 293K using specimens with a thickness of 2 mm.

Table 1. Chemical composition of selected steel (in wt.%).

C	Cr	Si	Mn	P	S	Ni	Cu
0.36	0.91	0.34	0.62	0.017	0.022	0.21	0.15

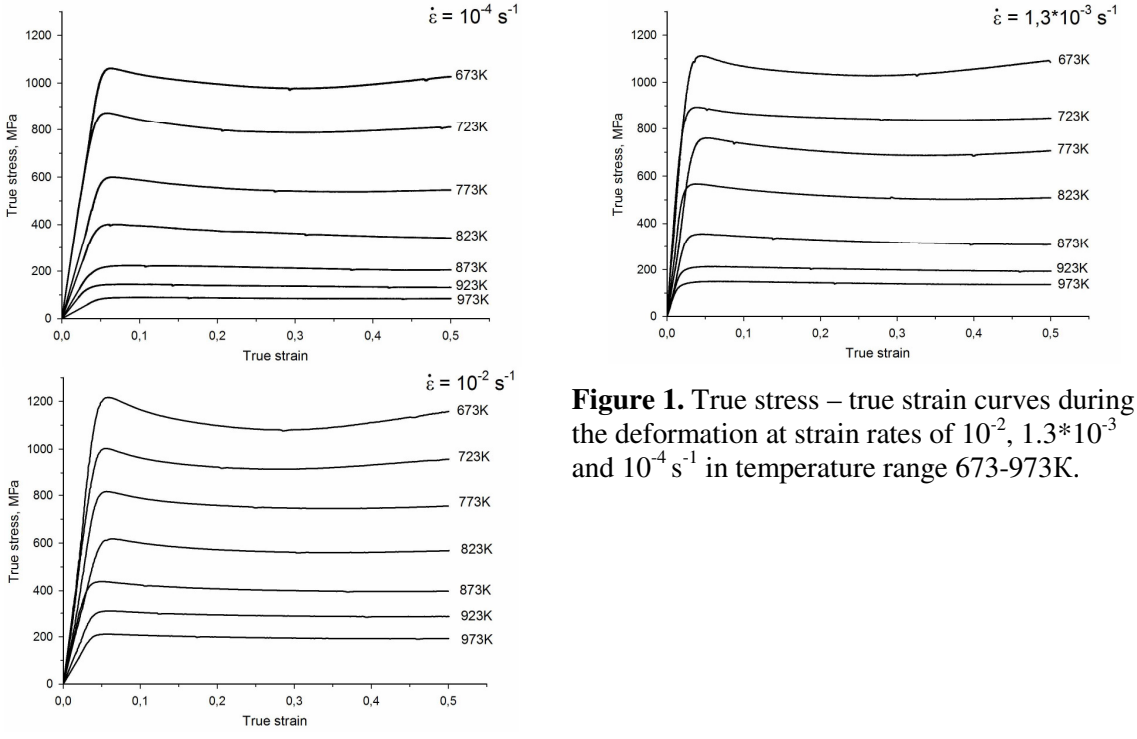

Figure 1. True stress – true strain curves during the deformation at strain rates of 10^{-2}, $1.3*10^{-3}$ and 10^{-4} s^{-1} in temperature range 673-973K.

3. Results and Discussion

3.1 Study of mechanical behavior during compression tests and determination of activation energy

The true stress – true strain curves obtained during compression testing in the temperature interval of 673-773K and different strain rates are shown on figure 1. The deformation behavior noticeably depends on temperature and strain rate, but the shape of the curves is typical for quenched medium-carbon steel samples subjected to compressive deformation [9, 10], so discuss it briefly. At all conditions a peak stress was observed at early stage of deformation. With a decrease in the strain rate and an increase in temperature, the peak became less pronounced. The maximum value of the peak stress corresponds to the temperature of 673K and strain rate 10^{-2} s^{-1} and is equal to 1216 MPa. Increase temperature without changing strain rate leads to peak stress decreasing to 212 MPa. At a strain rate $1.3*10^{-3}$ s^{-1} peak stress decreases with increasing temperature from 1137 to 156 MPa. At a strain rate 10^{-4} s^{-1} peak stress of 1063 MPa falls to 90 MPa. It also can be noted that with decrease of strain rate difference between the peak stress at temperatures of 673 and 973K tends to reduce. The pronounced steady-stage flow was observed at high temperatures, which can be connected with the occurrence of dynamic recovery and recrystallization.

Flow stress value at the strain of 0.4 was used for activation energy analysis as it approximately corresponds to steady state flow stage for all studied deformation condition. Dependence of the flow stress at the strain of 0.4 on the reverse temperature shows the presence of the critical temperature at which a change in the slope of average straight is observed, 823K. This indicates a change of controlling deformation mechanism. Therefore, the temperature range was divided into two intervals (673-823K and 873-973K) and the activation energy was determined for each of them.

The relationship between flow stress (σ) and strain rate ($\dot{\varepsilon}$) of plastic deformation can be described through Arrhenius type equation [11, 12]. At low stresses deformation behavior is characterized by a power law

$$\dot{\varepsilon} = A\sigma^n \exp(-\frac{Q}{RT}). \quad (1)$$

At high stress level there is a transition to an exponential law

$$\dot{\varepsilon} = A\exp(\beta\sigma)\exp(-\frac{Q}{RT}), \quad (2)$$

where $\dot{\varepsilon}$ is the strain rate (s^{-1}); σ – the flow stress (MPa), R – the universal gas constant (8.314 $J*mol^{-1}*K^{-1}$), T – the absolute temperature (K), Q – the activation energy of deformation ($kJ*mol^{-1}$); A, β, n are material constants.

The activation energy of plastic deformation in the temperature range 873-973K was determined using the equation 1. Taking the logarithm of Equation 1 and then partial differentiation for constant temperature gives

$$n = \left.\frac{\partial \ln(\dot{\varepsilon})}{\partial \ln\sigma}\right|_T, \quad (3)$$

and for constant strain rate

$$Q = Rn\left.\frac{\partial \ln\sigma}{\partial(1/T)}\right|_{\dot{\varepsilon}}. \quad (4)$$

Thus values of n and Q can be derived from the slope of the lines in the $\ln(\dot{\varepsilon})$ – $\ln\sigma$ and $\ln\sigma$ – $10^3/T$ plots. Value of the stress exponent n changes from n = 7.1 to n = 5.4 at temperatures of 873 and 973K respectively (figure 2a). To calculate the activation energy the average value of n = 6.3 was chosen. The activation energy of 378 kJ/mol is determined by averaging the values of Q at three different strain rates (figure 2b). This value of activation energy is much higher than the activation energy for

volume self-diffusion in α-iron, Q_l = 251 kJ/mol [11], however, comparable with previous studies for activation energy of plastic flow for ferrite [13, 14].

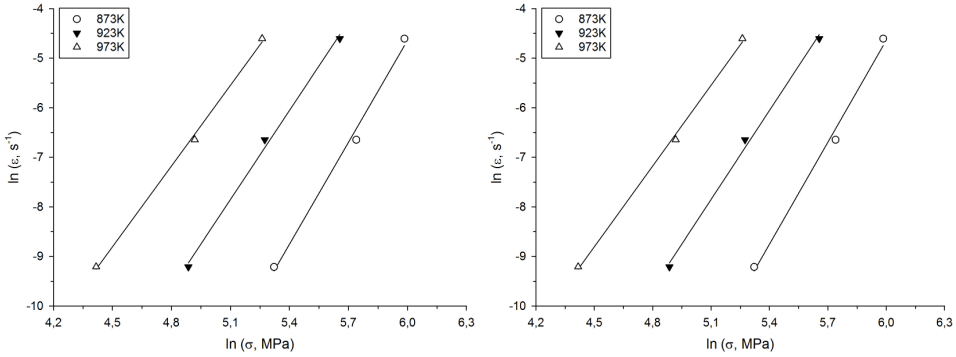

Figure 2. Relationships between $\ln(\dot{\varepsilon})$ – ln σ(a) and lnσ – 10^3/T (b) at strain 0.4.

At lower temperatures (673-823K) the activation energy was calculated according to the exponential law (equation 2). Taking the logarithm of both sides of equation 2 and then partial differentiation for constant temperature yields the following equation

$$\beta = \left.\frac{\partial \ln(\dot{\varepsilon})}{\partial \sigma}\right|_T , \tag{5}$$

and for constant strain rate

$$Q = R \left.\frac{\partial(\beta\sigma)}{\partial(1/T)}\right|_{\dot{\varepsilon}} . \tag{6}$$

Thus values of n and Q can be derived from the slope of the lines in the $\ln(\dot{\varepsilon})$ – σ and βσ – 10^3/T plots. Material constant β varies in the range 0.021-0.039 (figure 3a). The activation energy in the temperature interval 673-823K so is 563 kJ/mol by averaging the values of Q at three different strain rates. This value of the activation energy exceeds the activation energy at higher temperatures that probably can be connected with need of accounting of the threshold stress.

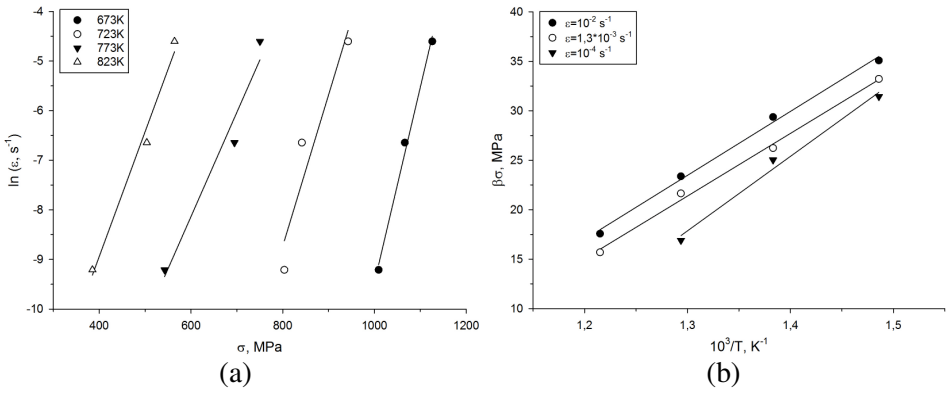

Figure 3. Relationships between $\ln(\dot{\varepsilon})$ – σ (a) and βσ – 10^3/T (b) at strain 0,4.

3.2 Microstructure evolution during compression tests

Microstructure of the steel after heating to deformation temperatures of 673, 773, 873 and 973K is shown in figure 4. At temperatures 673 and 773K a typical tempered martensitic structure was observed, in which prior-austenite grains are divided into packets that are subdivided into blocks of ferrite plates. It is seen that the thickness of the ferrite plates increases with temperature heating. At temperature 973K the formation of coarse ferritic grains free from sub-structure can be observed.

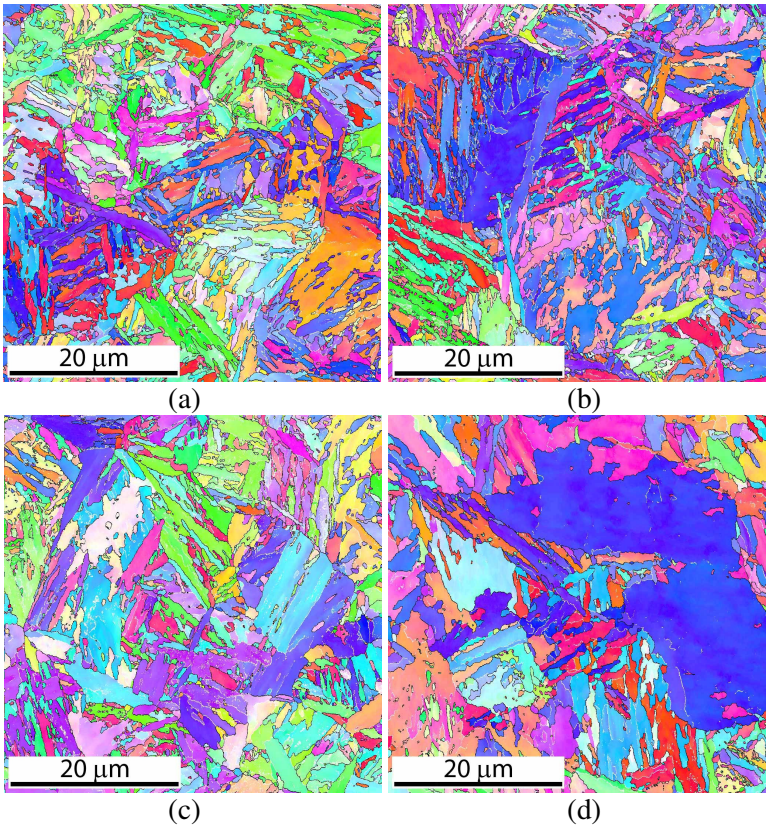

Figure 4. EBSD maps of the microstructure after heating to deformation temperatures of 673 (a), 773 (b), 873 (c) and 973K (d).

Figure 5 shows the microstructure after deformation at temperatures 673, 773, 873 and 973K to strains of $\varepsilon \sim 0.3$, 0.77 and 1.15 with strain rate of $1.3*10^{-3}$ s^{-1}. It is seen that the microstructure strongly depends on temperature and strain. As strain increases the reduction in the thickness of ferritic grains is observed at all temperatures. The grains become significantly elongated in direction perpendicular to the compression axis. This is most noticeable at low temperatures of 673 and 773K, when an average ferrite grain thickness is gradually reduced to 190 and 200 nm at the strain of 1.15, respectively. With increasing deformation temperature to 873K fine equiaxed grains appear inside elongated grains. Increase of the deformation temperature up to 973K leads to a formation of equiaxed microstructure probably due to dynamic recrystallization which is the main mechanism of microstructural formation at elevated temperatures.

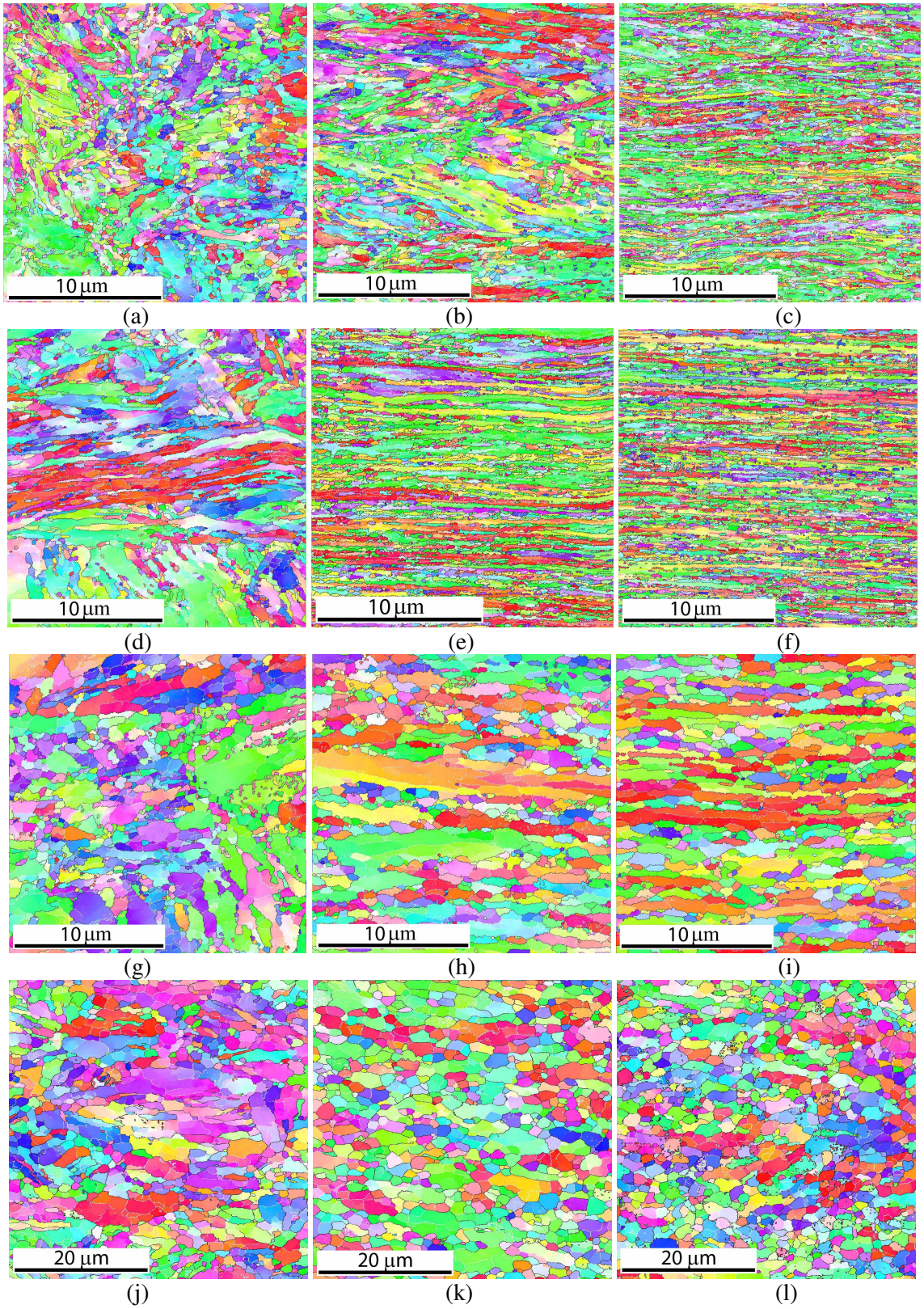

Figure 5. EBSD maps of the microstructure after deformation with strain rate of $1.3*10^{-3}$ s^{-1} at temperatures 673 (a-c), 773 (d-f), 873 (g-i) и 973K (j-l) to strain ε ~ 0.3, 0.77 and 1.15. The compression axis in the images corresponds to the vertical direction.

Dependencies of HABs fraction, HABs spacing and aspect ratio on strain at different temperatures at strain rate of $1.3*10^{-3}$ s^{-1} obtained from EBSD maps are given in figures 6 and 7. It should be noted that HABs fraction of specimens heated to deformation temperatures, i.e. in condition prior to compression, changes non-monotonously (figure 6). With increase of the temperature from 673 to 873K HABs fraction decreases remarkably from about 75% to 60% and then rises to 75% back at T = 973K. Such a change is caused by development of two processes: decrease is caused by recovery, operating at low temperatures, which reduces HABs fraction due to formation of low angle boundaries, and increase of HABs fraction at 973K is caused by static recrystallization. Non-monotonic dependence of HAB fraction on strain during compression at all temperatures except temperature of 873K is found. At temperature of 673K HAB fraction decreases rapidly at early stages of deformation and slightly increases during following straining. However HABs fraction even at maximum strain of 1.1 is lower than in the specimen heated to deformation temperature because of development of substructure. At temperatures of 773 and 973K HABs fraction shows significant growth after the initial fall due to development of dynamic recrystallization. Monotonic increase of the HABs fraction at 873K is a result of competition between the substructure formation and dynamic recrystallization.

As the HABs spacing (thickness of ferrite grains) shows monotonic decrease with increasing strain at each temperature (figure 7a) one can expect that aspect ratio i.e. ratio between the length and thickness of the grains will show a monotonic increase, since the deformation scheme by compression involves grains elongation perpendicular to the deformation axis. However, the dependencies of aspect ratio on true strain at different temperatures are more complicated (figure 7b). At 673K aspect ratio decreases at the early stages of deformation but then remarkable growth occurs. At 773K another relationship is found. When strain increases to 0.3 significant rise of aspect ratio happens then followed by stagnation. This may be result of the limited "field of view" of the produced EBSD maps which restricts the analysis of grains with length more than 20 μm. Similar behavior is observed at 873K, however aspect ratio is lower than at 773K. The aspect ratio during deformation at 973K decreases with increase of strain, which is associated with an increase in the fraction of equiaxed grains due to dynamic recrystallization.

Thus summarizing the obtained results the presence of two temperature ranges with different mechanisms controlling the structure formation is found. At low temperatures 673-773K the main process is geometrical effect of deformation, reflected in a strong decrease of the thickness of the ferrite grains. When the temperature rises to 873-973K dynamic recrystallization becomes dominant and reasonably equiaxed grains are formed. However, the peculiarities of microstructure formation at each temperature are rather complex, and one might suggest that initial microstructure (i.e. microstructure of the specimen after heating at deformation temperature) plays an important role. Finally, for formation of EFG structure deformation at temperatures of 673-773K should be preferred.

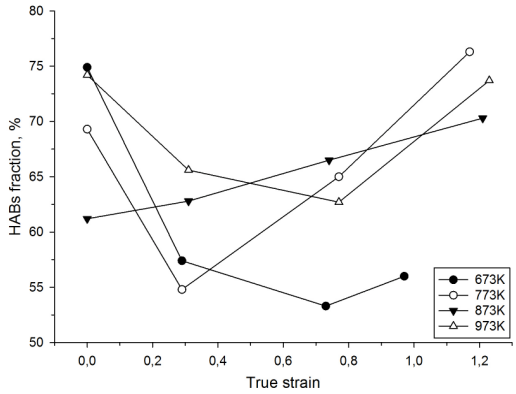

Figure 6. Dependence of HABs fraction on strain during compression tests at different temperatures.

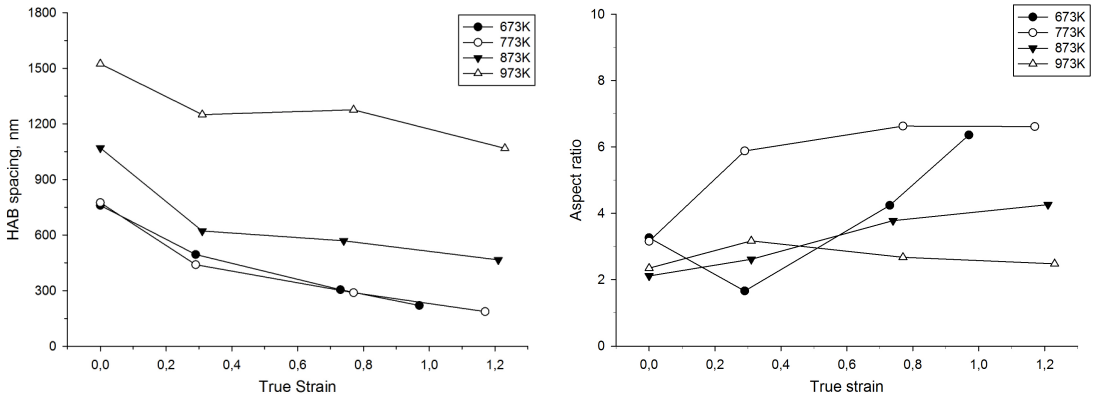

(a) (b)

Figure 7. Average statistical data obtained from EBSD maps, showing (a) the transverse HABs spacing and (b) the grain aspect ratio as a function of strain at different temperatures.

3.3 Microstructure and mechanical properties of elongated fine grained steel produced by caliber rolling

As it was noted above the temperature of changing the main mechanism controlling structure formation is 823K. It is intriguing to study the microstructure and properties of steel produced by deformation involving different mechanisms of microstructure formation. Thus two deformation temperatures for caliber rolling of steel of 773 and 873K corresponding to ± 50K from the critical temperature of 823K were chosen. Figure 9 shows the EBSD maps in a longitudinal section of rod rolled to strain of 1.1 at both temperatures. The aspect ratio is equal to 4 and 6 at temperatures 773 and 873K, respectively. The HABs fraction is equal to 55% and 61% at temperatures 773 and 873K, respectively.

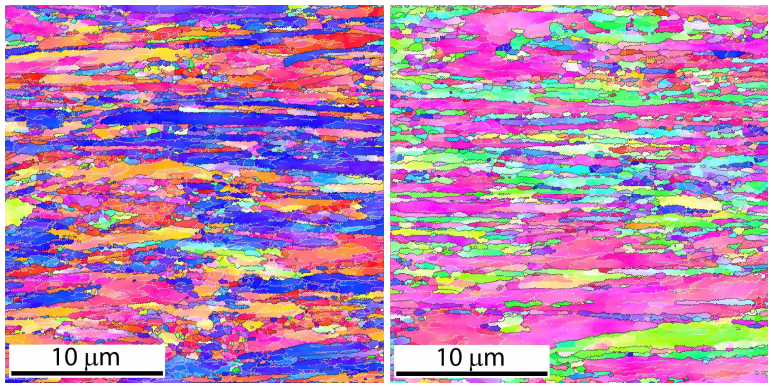

(a) (b)

Figure 9. EBSD in a longitudinal section of steel rod after rolling at temperatures 773 (a) and 873 (b) at strain ε ~ 1.1.

The tensile properties of steel after rolling were studied at room temperature (table 2). The results were compared to properties of steel after quenching and tempering. EFG structure formation results in noticeable changes in the mechanical properties. Yield strength increases from 840 MPa after quenching and tempering at 773 K to 1150 MPa after rolling at 773 K, and from 635 MPa to 885 MPa – after same treatments at 873 K. Ultimate tensile strength increases from 980 MPa to 1200 MPa after treatment at 773 K and from 805 MPa to 925 MPa – at 873K. However, strengthening is accompanied by some loss of ductility. Elongation to failure considerably decreases after rolling at 773 K from

17.2% to 11.9%. Rolling at 873K results in insignificant change in elongation value which decreases from 21.7% to 19.4%.

Table 2. Mechanical properties of medium-carbon steel after heat treatment: quenching and tempering, and rolling

Sample name	Yield strength, MPa	Ultimate tensile strength, MPa	Elongation, %
Quenching and tempering at 773K, 1h	840	980	17.2
Rolling at 773K, ε ~1.1	1150	1200	11.9
Quenching and tempering at 873K, 1h	635	805	21.7
Rolling at 873K, ε ~1.1	885	925	19.4

The results of the impact tests at different temperatures are shown in table 3. As not all samples were fractured during test, therefore the value of impact energy was used as a measure of the impact toughness. One could note that the dependence of impact energy has rather unusual dependence on temperature. No sharp changes in impact energy were found when the temperature decreased. This kind of behavior can be attributed to small scale of the samples, used in this study. Nevertheless it is clearly seem that impact energy of samples after heat treatment was remarkably lower than that after rolling at all test temperatures. Impact energy after rolling was about 1.5 times higher than after quenching and tempering.

Table 3. Impact energy of samples of medium-carbon steel after heat treatment: quenching and tempering, and rolling

	Impact energy, J						
Test temperature, K	293	273	253	233	208	173	93
Quenching and tempering at 773K, 1h	7.5	7.8	7.2	7.0	7.0	6.6	5.7
Rolling at 773K, ε ~1.1	11.7	10.9	10.5	11.5	11.6	9.8	9.9
Quenching and tempering at 873K, 1h	9.1	9.6	8.4	9.8	9.2	8.4	8.1
Rolling at 873K, ε ~1.1	12.2	12.7	12.1	11.8	12.8	12.8	11.6

4. Conclusions

The influence of temperature in range of 673-973K and strain rate on the EFG structure formation and its effect on mechanical properties of medium-carbon steel was investigated. The following results were obtained.

1. Presence of two intervals at temperatures 673-973K, which are characterized by different mechanisms, mainly controlling the formation of the microstructure in steel was revealed through compression test. At the low temperature range (673-823K) the formation of the structure is governed by geometric effect of the deformation and at high temperatures (873-973K) the dynamic recrystallization becomes dominant process.

2. Noticeable changes in the mechanical properties of the steel after rolling at 773-873K as compared with the properties after quenching and tempering were found: yield strength increased from 840 MPa after quenching and tempering at 773 K to 1150 MPa after rolling at 773 K, and from 635 MPa to 885 MPa – at 873 K. Ultimate tensile strength increased from 980 MPa to 1200 MPa at 773 K and from 805 MPa to 925 MPa – at 873K. The impact energy of samples after rolling was on average 1.5 times higher than after quenching and tempering at all test temperatures.

References

[1] Bhadeshia H, Honeycombe R 2006 *Steels: Microstructure and Properties Third edition* (Elsevier: Butterworth-Heinemann) p 306
[2] Song R, Ponge D, Raabe D, SpeerJ D, Matlock D K 2006 *Mater. Sci. Eng. A* **441** 1-17
[3] Kimura Y, Inoue T, Yin F, Tsuzaki K 2008 *Science* **320** 1057-59
[4] Kimura Y, Inoue T, Yin F, Tsuzaki K 2010 *ISIJ Int.* **50** 152-161
[5] Kimura Y, Inoue T 2013 *Metall. Mater. Trans. A* **44** 560-576
[6] Ryan N D, McQueen H J 1986 *J. Mech. Work. Tech.* **12** 323-349
[7] Cabrera J M, Omar A Al, Jonas J J, Prado J M 1997 *Metall. Mater. Trans. A* **28** 2233-44
[8] McQueen H J, Ryan N D 2002 *Mater. Sci. Eng. A* **322** 43-63
[9] Zhao X, Yang X, Jing T 2012 *J. Iron Steel Res. Int.* **19(8)** 75-78
[10] Hase K, Tsuji N 2011 *Scripta Mater.* **65** 404-407
[11] Frost H J, Ashby M F 1982 *Deformation-Mechanism Maps: The plasticity and Creep of Metals and Ceramics* (Pergamon Press) p 166
[12] Cadek J 1988 *Creep in Metallic Materials* (Elsevier)
[13] Lourenço N J, Jorge Jr A M, Rollob J M A, Balancin O 2001 *Materials Research* **4** 149-156
[14] Girish Shastry C, Parameswaran P, Mathew M D, Bhanu Sankara Rao K, Mannan S L 2007 *Mater. Sci. Eng. A* **465** 109-115